International Journal of Thermophysics, Vol. 16, No. 2, 1995

Study of Flow in a Smectic Liquid Crystal in the X-Ray Surface Forces Apparatus[1]

S. H. J. Idziak,[2,3] I. Koltover,[2,3,4] K. S. Liang,[5]
J. N. Israelachvili,[3,6] and C. R. Safinya[2,3,4,7]

We describe the newly invented X-Ray Surface Forces Apparatus (X-SFA) which allows the simultaneous measurement of forces and collective structures of confined complex fluids under static and flow conditions. The structure of the smectic liquid crystal 8CB (4-cyano-4'-octylbiphenyl) confined between two mica surfaces with separation ranging from 4000 to 20,000 Å was measured. At small gaps and no shear, the smectic layers take on distinct stable orientations, including the bulk forbidden "*b*" orientation, which persist under low shear ($\dot{\gamma} \leqslant 30\ \mathrm{s}^{-1}$). However, at higher shear rates ($\dot{\gamma} = 360\ \mathrm{s}^{-1}$), the shear acts to dramatically order and align the smectic layers into a single "*a*" orientation.

KEY WORDS: confinement; SFA; Surface Forces Aparatus; X-Ray Surface Forces Apparatus; XSFA.

1. INTRODUCTION

Under most experimental or practical circumstances, the bulk properties of small-molecule fluids under flow can be described with the classical theory of Newtonian hydrodynamics [2]. However, in complex fluids that manifest some larger scale dimension, such as colloidal suspensions, polymeric solutions, and liquid crystals, this classical theory breaks down

---

[1] Paper presented at the Twelfth Symposium on Thermophysical Properties, June 19-24, 1994, Boulder, Colorado, U.S.A.

[2] Materials Department, University of California, Santa Barbara, California 93106, U.S.A.

[3] Materials Research Laboratory, University of California, Santa Barbara, California 93106, U.S.A.

[4] Physics Department, University of California, Santa Barbara, California 93106, U.S.A.

[5] Exxon Research & Engineering Company, Annandale, New Jersey 08801, U.S.A.

[6] Department of Chemical Engineering, University of California, Santa Barbara, California 93106, U.S.A.

[7] Author to whom correspondence should be addressed.

0195-928X/95/0300-0299$07.50/0 © 1995 Plenum Publishing Corporation

and new normal stress terms must be introduced into the hydrodynamic equations. Weissenberg [3] was among early workers to apply these normal stress terms in a study of surfactant solutions under flow. The effects of flow in complex fluid systems are of high technological importance, such as in the area of spinning of polymer fibers [4, 5].

X-ray diffraction studies have proven useful in the study of complex fluids under flow. The liquid crystal 8CB (4-cyano-4′-octylbiphenyl), which forms both a smectic and a nematic phase close to room temperature, has been studied with an X-Ray Couette Shear Cell [6]. With this technique, and following the notation of Meicowicz [7] (see Fig. 1A), it was determined that the sheared smectic phase took on either the "*a*" orientation, in

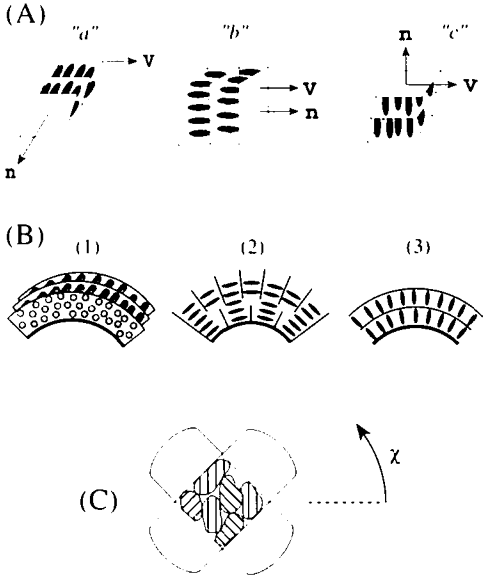

Fig. 1. (A) Description of the real-space orientations of a smectic liquid crystal under flow, following the notation due to Meicowicz [7]. ("*a*") The layer normal is along the z direction; ("*b*") the layer normal lies along the shear direction resulting in the deformation of the layers under flow; and ("*c*") the layer normal is along the velocity gradient, allowing the layers to slide over each other. (B) Sketch of the three possible orientations of the smectic layers along a curved surface. (C) Model of the layer orientations seen in 8CB between two hard surfaces with a 5000-Å separation showing the three distinct orientations discussed in the text.

which the individual molecules are free to roll over each other, or the "*c*" orientation, where the layers can slide freely over each other. The "*b*" orientation, which implies the breakdown of the smectic layers, was never observed.

In contrast with the nonequilibrium effects of flow, confinement of a sample between two surfaces produces strong equilibrium constraints on the structure [8]. These include changes in the collective structure of the trapped molecules in simple or complex fluids of molecular aggregates such as polymers, vesicles, biomembranes, or colloidal suspensions in a liquid [8–13]. The density and structural order in these types of systems have also been shown to change by molecular dynamics simulations [14]. This is especially true as the confinement gap is decreased down to an inherent length scale in the system, such as a molecular size. The effects of confinement in porous media have been studied with spectroscopic (see, e.g., Ref. 12), calorimetric [13], and neutron diffraction [15] techniques. The Surface Forces Apparatus (SFA) has been used to measure friction, direct force, and rheological properties of fluids confined in a well-characterized gap [8–10]. The newly developed X-Ray Surface Forces Apparatus (X-SFA) [1, 16] has recently been used to image directly the collective structure of a confined complex fluid with a well-known gap for the first time. This apparatus is the only current technique that can be used to image directly a confined complex fluid and is not destructive to the sample.

In this paper, we will discuss the details of performing experiments with the X-SFA, including a description of newly designed surfaces which greatly reduce the background scattering levels measured during the experiment. We will then discuss some results we have obtained using this device to study 8CB under flow and confinement.

2. EXPERIMENTS

The x-ray diffraction experiments were conducted at the multipole wiggler beamlines 6-2 and 10-2 at the Stanford Synchrotron Radiation Laboratory (SSRL). A Si(111) monochromator was used to select an 8-keV x-ray beam focused on the sample position. This beam was further defined by a 125-μm pinhole located a few inches from the sample. Diffraction patterns were then measured either with a Bicron scintillation detector providing one-dimensional diffractograms, or a 180-mm-diameter MAR image plate two-dimensional detector.

The X-SFA is based on the conventional Surface Forces Apparatus (Mk III) [17]. This apparatus allows the gap between two atomically smooth surfaces to be adjusted from a few angstroms to several microns with angstrom resolution. A photograph of the X-SFA is shown in Fig. 2.

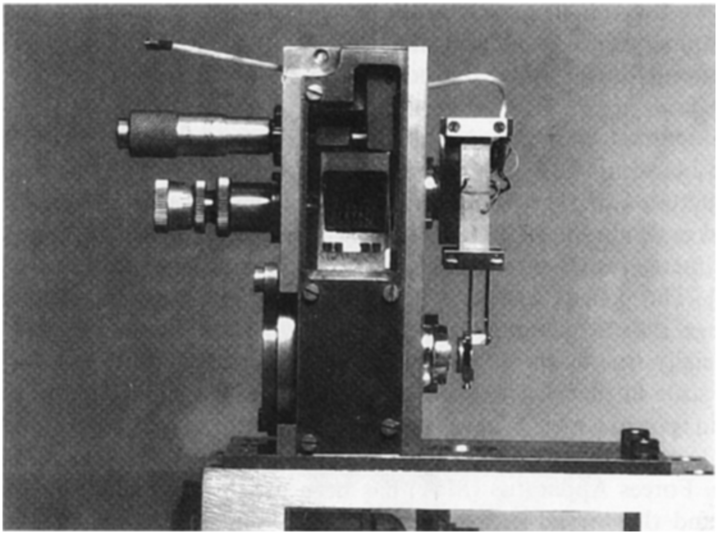

Fig. 2. Photograph of the X-Ray Surface Forces Apparatus as described in the text.

The surfaces typically used in the SFA are made of solid glass cylindrical lenses that have been covered with atomically smooth cleaved mica. The curvature of each surface allows a single point of contact to be created between the two surfaces. The surfaces in the X-SFA were modified to allow direct x-ray access to the confined sample. Two different types of surfaces were developed for these experiments, which we refer to as a hard surface and a soft surface.

The hard surface is schematically illustrated in Fig. 3A. These surfaces are constructed from 2-mm-diameter, thin-walled quartz capillary tubes, to which the cleaved mica is glued. An x-ray beam must then pass in transmission through the four glass surfaces, two mica surfaces, as well as the glue bonding the mica to the glass. To minimize the effects of scattering from the glass and glue, we have recently developed the "soft" surfaces shown in Fig. 3B. Here, conventional cylindrical lenses with a radius of 20 mm have a tapered hole drilled through them to allow x-ray access. The holes are then covered with a thin mica sheet. This then eliminates any scattering contribution from the glass and glue seen in the hard-surface technique; the only background scattering is due to the single-crystal mica surfaces, which is well understood. Shear is performed on the sample by continuously sliding one surface with respect to the other using an oscillatory motion.

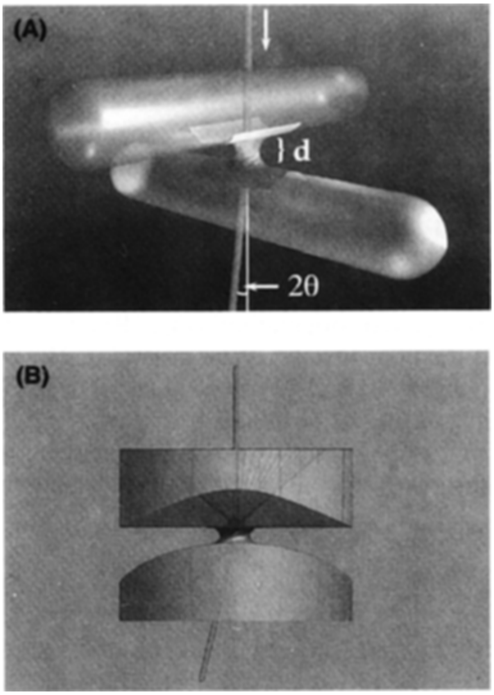

Fig. 3. (A) Sketch of the two crossed cylinders that are used to form the hard surfaces described in the text. The path of the x-ray beam in transmission through the two mica surfaces and the sample can be seen. (B) Drawing of the two discs used in the soft-surface experiments.

3. DISCUSSION

Diffraction results from the experiments conducted with 8CB confined by the hard surfaces are summarized in Fig. 4, which shows the alignment observed in the "*a*"–"*b*" plane with a 4000-A gap. The rotation angle χ corresponds to the angle by which the surfaces have been rotated about the incident x-ray beam as shown in Fig. 1C. The long axes of the surfaces are oriented at $\chi = \pm 45^\circ$. Figure 4C shows the order present with no shear acting on the sample; it can be seen that the smectic layers are ordered in three discrete orientations, $\chi = \pm 45^\circ$ and $\chi = 0^\circ$, with the layer normals pointing either along each cylindrical axis or at a 45° angle to the axis. These orientations are shown in Fig. 1C. When the top surface is sheared with respect to the bottom surface, the diffractograms seen in Fig. 4A and B are observed. Clearly, the results obtained at zero shear and at $\dot{\gamma} = 30\ \mathrm{s}^{-1}$ are qualitatively the same; no major structural rearrangements have occurred at these low shear rates. The bulk-flow forbidden "*b*" orientation persists at $\dot{\gamma} = 30\ \mathrm{s}^{-1}$; the effects of confinement are dominating those one would expect from flow at these low shear rates, based on the Couette Flow Cell experiments [6]. However, there is evidence of a peak starting to emerge at $\chi = 90^\circ$ (see Fig. 4), which indicates the onset of the "*a*" orientation.

A schematic of the free orthogonal orientations of the liquid crystal molecules on the curved mica surface is shown in Fig. 1B. For a single curved surface, the planar orientation (Fig. 1B1) with **n** parallel to the cylinder axis, and the homeotropic orientation (Fig. 1B3) with **n** normal to the surface, involve small (Fig. 1B3) or no (Fig. 1B1) elastic distortion. The planar orientation with **n** perpendicular to the cylinder axis (Fig. 1B2) requires the creation of dislocations and should therefore be least favorable. With two opposing and crossed surfaces, both planar and homeotropic

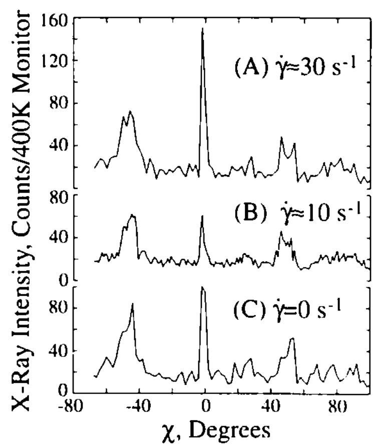

Fig. 4. X-ray orientational scans showing the discrete planar molecular configurations. (A) The shear rate $\dot{\gamma}$ is $30\ \mathrm{s}^{-1}$. (B) $\dot{\gamma} = 10\ \mathrm{s}^{-1}$. (C) $\dot{\gamma} = 0$ (cylinders are stationary). The "*a*" orientation (see Fig. 1A) corresponds to χ being roughly $\pm 90^\circ$; the "*b*" orientation to $\chi \approx 0^\circ$. The shearing velocity was in the plane of scattering at χ approximately 0°. Each point was counted for approximately 17 s. The point spacing in B is 1°, while the point spacing in A and C is 2°.

orientations will involve elastic distortions to satisfy the two surfaces simultaneously. The precise orientations to be chosen will involve the magnitude of the elastic constants. The mica sheet prefers that the 8CB molecules lie parallel with the surface, in the planar alignment [11, 18]. Experimentally, we observe domains (Fig. 1C) with orientations consistent with the planar orientation shown in Fig. 1B1 where the long axis of the molecules points along the cylinder axis. This orientation gives the diffraction peaks seen at $\chi = \pm 45°$. The "*b*" orientation seen at $\chi = 0°$ is probably due to flow alignment occurring while the sample is being loaded.

Results derived from experiments using soft surfaces are shown in Fig. 5. Two-dimensional x-ray diffractograms are shown in Fig. 5A for

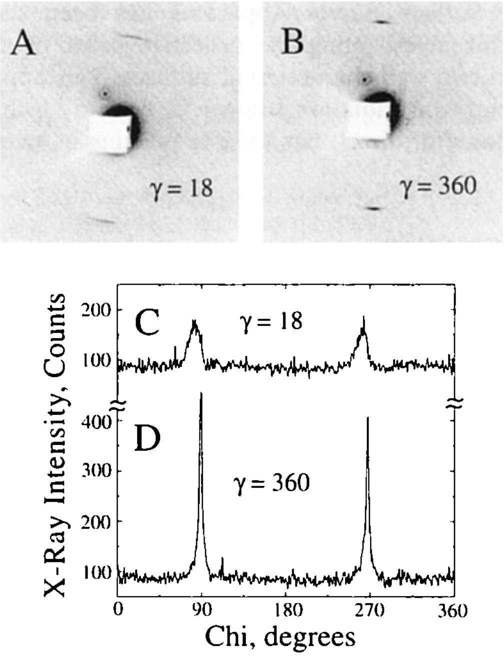

Fig. 5. Two-dimensional x-ray diffraction patterns showing the alignment seen in the X-SFA with 8CB confined in a gap of 8000 A at very low ($\dot{\gamma} = 18\ s^{-1}$) shear (A) and a shear rate of 360 s^{-1} (B). The white square at the center of each image is the beam stop; the dark spot just above is the center of the 2D detector. One-dimensional orientational scans derived from these images are shown for very low shear (C) and shear (D), showing the high degree of orientation and alignment obtained through the shearing process. Each two-dimensional scan was exposed for 20 min.

the case of very low shear ($\dot{\gamma} = 18\ \mathrm{s}^{-1}$) and in Fig. 5B for a shear rate of $360\ \mathrm{s}^{-1}$ (note that this shear rate is 20 times larger than the one obtained during the hard-surface experiments). Also note that the 18-s^{-1} shear rate is still in the range that did not affect the orientational order in the hard-surface experiments. One-dimensional orientational scans derived from these images are presented in Figs. 5C and 5D, respectively. It can clearly be seen that the applied shear significantly orders the sample, reducing its mosaic from 15° to less than 4°, indicating a very high degree of alignment. Also, the shear changes the orientation of the layers into the pure "*a*" orientation that was observed in the bulk flow experiments. This "*a*" orientation can also be seen emerging in the hard-surface experiments at lower shear rates.

The X-Ray Surface Forces Apparatus has been shown to be an invaluable tool for investigating the collective order of a complex fluid confined between two well-characterized surfaces. This apparatus, coupled with bright synchrotron radiation sources, is the only technique currently available that allows for direct, noninvasive imaging of a confined complex fluid.

ACKNOWLEDGMENTS

We gratefully acknowledge conversations with Robijn Bruinsma. C.R.S. and J.N.I. gratefully acknowledge partial support by the Office of Naval Research under grant N00014-93-1-0269. C.R.S. is grateful for partial support of an Exxon Education Grant. The synchrotron x-ray scattering experiments described in this paper were carried out on beam lines 6-2 and 10-2 at the Stanford Synchrotron Radiation laboratory, which is supported by the U.S. Department of Energy. The Materials Research Laboratory at Santa Barbara is supported by NSF under grant No. DMR-9123048.

REFERENCES

1. S. H. J. Idziak, C. R. Safinya, R. S. Hill, M. Ruth, H. E. Warriner, K. E. Kraiser, K. S. Liang, and J. N. Israelachvili, *Science* **264**:1915 (1994).
2. G. K. Batchelor, *An Introduction to Fluid Dynamics* (Cambridge University Press, Cambridge, 1967).
3. K. Weissenberg, *Nature* **159**:310 (1947).
4. C. Bastiaansen, H. W. Schmidt, T. Nishino, and P. Smith, *Polymer* **34**(18):3951 (1993).
5. J. R. A. Pearson, *Mechanics of Polymer Processing* (Elsevier Applied Science, London, 1985).
6. C. R. Safinya, E. B. Sirota, and R. Plano, *Phys. Rev. Lett.* **66**:1986 (1991); C. R. Safinya, E. B. Sirota, R. Plano, R. F. Bruinsma, C. Jeppesen, R. J. Plano, and L. J. Wenzel, *Science* **261**:588 (1993).

7. M. Miecowicz, *Nature* **158**:27 (1946).
8. J. N. Israelachvili, *Intermolecular and Surface Forces*, 2nd ed. (Academic Press, New York, 1991).
9. J. Van Alsten and S. Granick, *Phys. Rev. Lett.* **61**:2570 (1988).
10. J. Klein, D. Perahia, and S. Warburg, *Nature* **352**:143 (1991); J. N. Israelachvili, A. M. Homola, and P. M. McGuiggan, *Science* **240**:189 (1988).
11. J. Als-Nielsen, in *Topics in Current Physics*, W. Schommers and P. V. Blackenhagen, eds. (Springer-Verlag, Berlin, 1987), p. 181; P. S. Pershan, *J. Phys. Coll.* (Paris) **50**:C7-1 (1989); B. Jerome, *Rep. Prog. Phys.* **54**:391 (1991) and references therein.
12. J. M. Drake and J. Klafter, *Phys. Today* **43**(5):46 (1990) and references therein; J. M. Drake, J. Klafter, and P. Levitz, *Science* **251**:1574 (1991).
13. T. Bellini, N. A. Clark, C. D. Muzny, and L. Wu, *Phys. Rev. Lett.* **69**:788 (1992).
14. M. Schoen, D. J. Diestler, and J. H. Cushman, *J. Chem. Phys.* **87**:5464 (1987); C. L. Rhykerd, Jr., M. Schoen, D. J. Diester, and J. H. Cushman, *Nature* **330**:461 (1987); P. A. Thompson, M. O. Robbins, and G. S. Grest, *Phys. Rev. Lett.* **68**:3448 (1992).
15. M. Y. Lin, S. K. Sinha, J. M. Drake, X.-I. Wu, P. Thiyagarajan, and H. B. Stanley, *Phys. Rev. Lett.* **72**:2207 (1994).
16. S. H. J. Idziak, C. R. Safinya, E. B. Sirota, R. F. Bruinsmaa, K. S. Liang, and J. N. Israelachvili, in *ACS Symposium Series No. 578, Structure and Flow in Surfactant Solutions*, C. A. Herb and R. K. Prud'homme, eds. (ACS, Washington, D.C., 1994), Chapter 20.
17. J. N. Israelachvili and P. M. McGuiggan, *J. Mater. Res.* **5**(10):2223 (1990).
18. P. Pieranski and B. Jerome, *Phys. Rev. A* **40**:317 (1989).